Discovering the Electromagnetic Counterparts of Binary Neutron Star Mergers with WFIRST

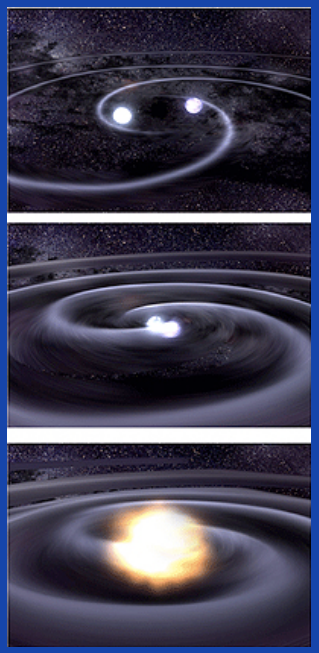

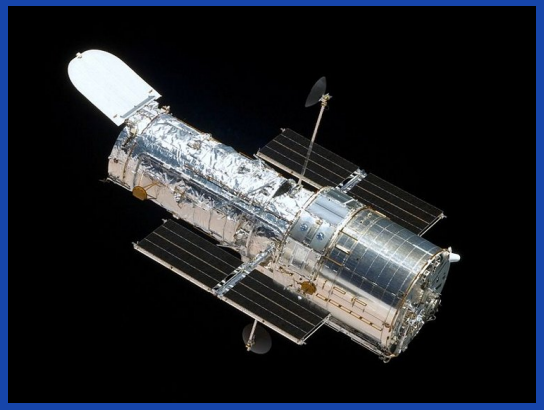

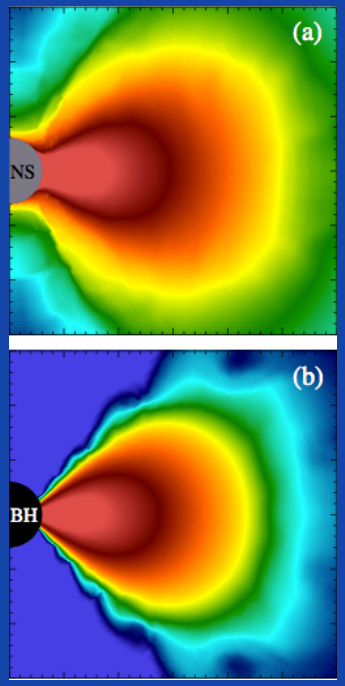

Brian Metzger

Columbia University

Rodrigo Fernandez, Dan Kasen, Eliot Quataert (UC Berkeley)

Edo Berger, Wen-Fai Fong (Harvard), Tony Piro (Caltech)

Almudena Arcones, Gabriel Martinez-Pinedo (GSI/TU Darmstadt)

Andreas Bauswein (U Thessaloniki), Stephane Goriely (U Brussels)

WFIRST: Science and Techniques, Pasadena, November 17, 2014

Gravitational Waves from Binary NS Mergers

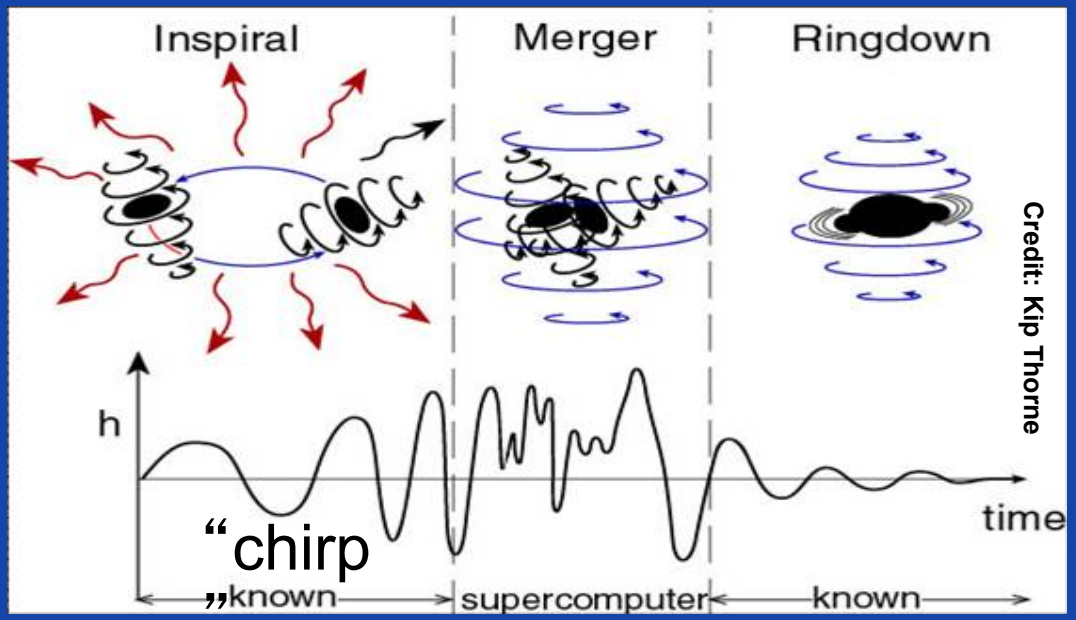

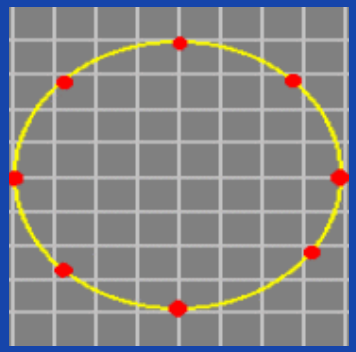

Ground Interferometers

LIGO 6th Science Run
(2010) Range ~ 20-50 Mpc

"Advanced" LIGO+Virgo
(~2017) Range ~ 200-500 Mpc

Detection Rate ~ 1-100 yr^{-1}

LIGO (North America)

Virgo (Europe)

Importance of EM Detection:

- Improve "confidence" in GW detection; dig deeper into GW data
- Independently constrain binary parameters
- Astrophysical context (e.g. host Galaxy & environment)
- Cosmology (e.g. H_0, w); test strong-field GR; constrain neutron star EOS

Example: Origin of R-Process Nuclei

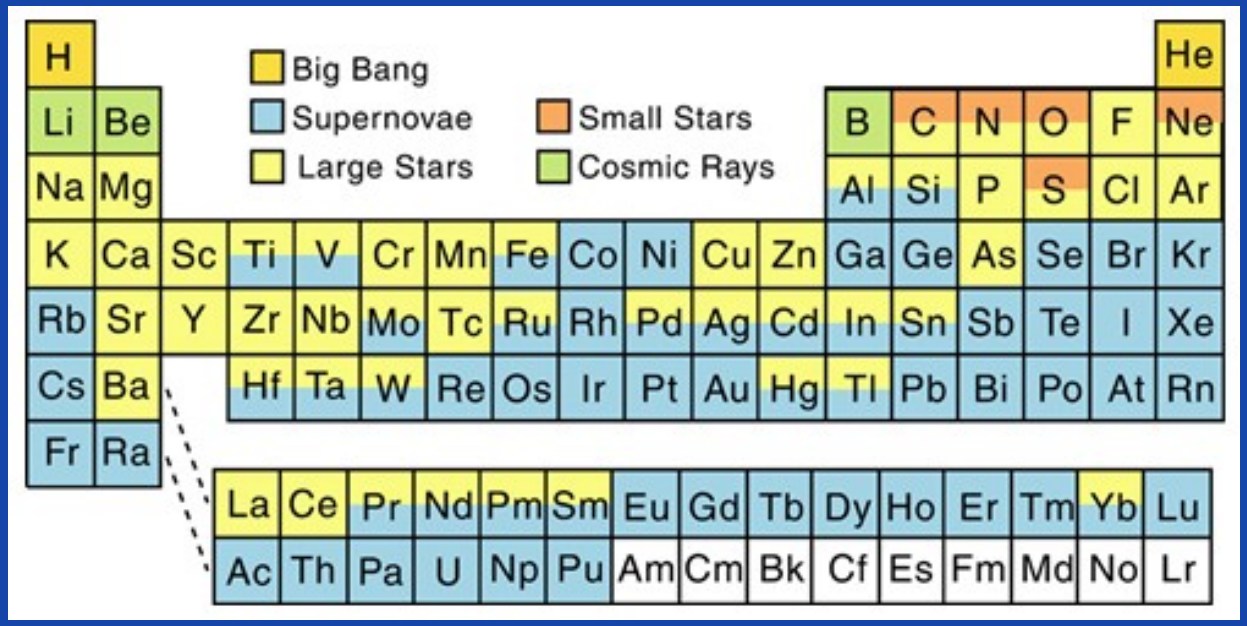

Core Collapse Supernovae or NS Binary Mergers?

Origin of R-Process Nuclei

Core Collapse Supernovae or NS Binary Mergers?

Galactic r-process rate:

$$\dot{M}_{A>130} \sim 5 \times 10^{-7} M_{\odot}\ \mathrm{yr}^{-1}$$

(Qian 2000)

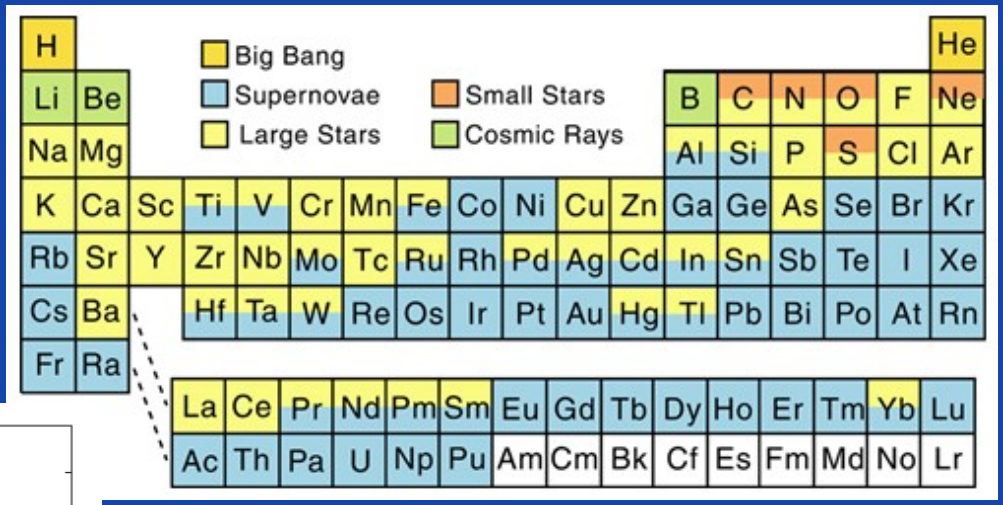

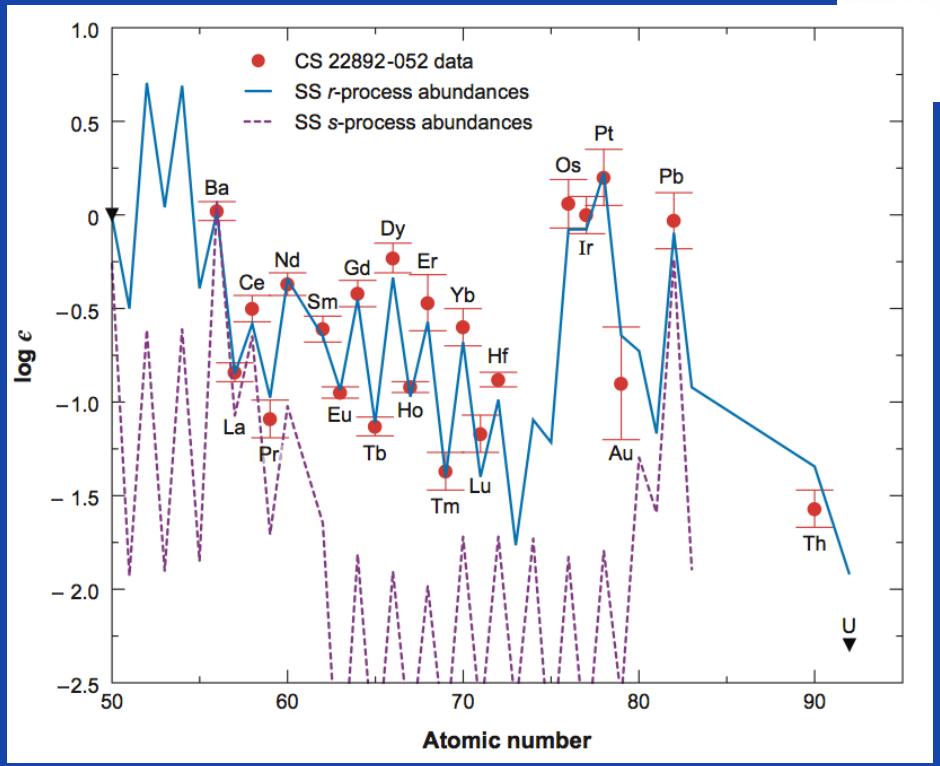

Snedan, Cowan & Gallino 2008

fraction of r-process from NS mergers:

$$f_R \sim \left(\frac{\dot{N}_{\mathrm{merge}}}{10^{-4}\ \mathrm{yr}^{-1}}\right)\left(\frac{\overline{M}_{\mathrm{ej}}}{10^{-2} M_{\odot}}\right)$$

Importance of EM Detection:

- Improve “confidence” in GW detection; dig deeper into GW data
- Independently constrain binary parameters
- Astrophysical context (e.g. host Galaxy & environment)
- Cosmology (e.g. H_0, w); test strong-field GR; constrain neutron star EOS

Sky Error Regions ~ 10-100 deg^2 (~2019)

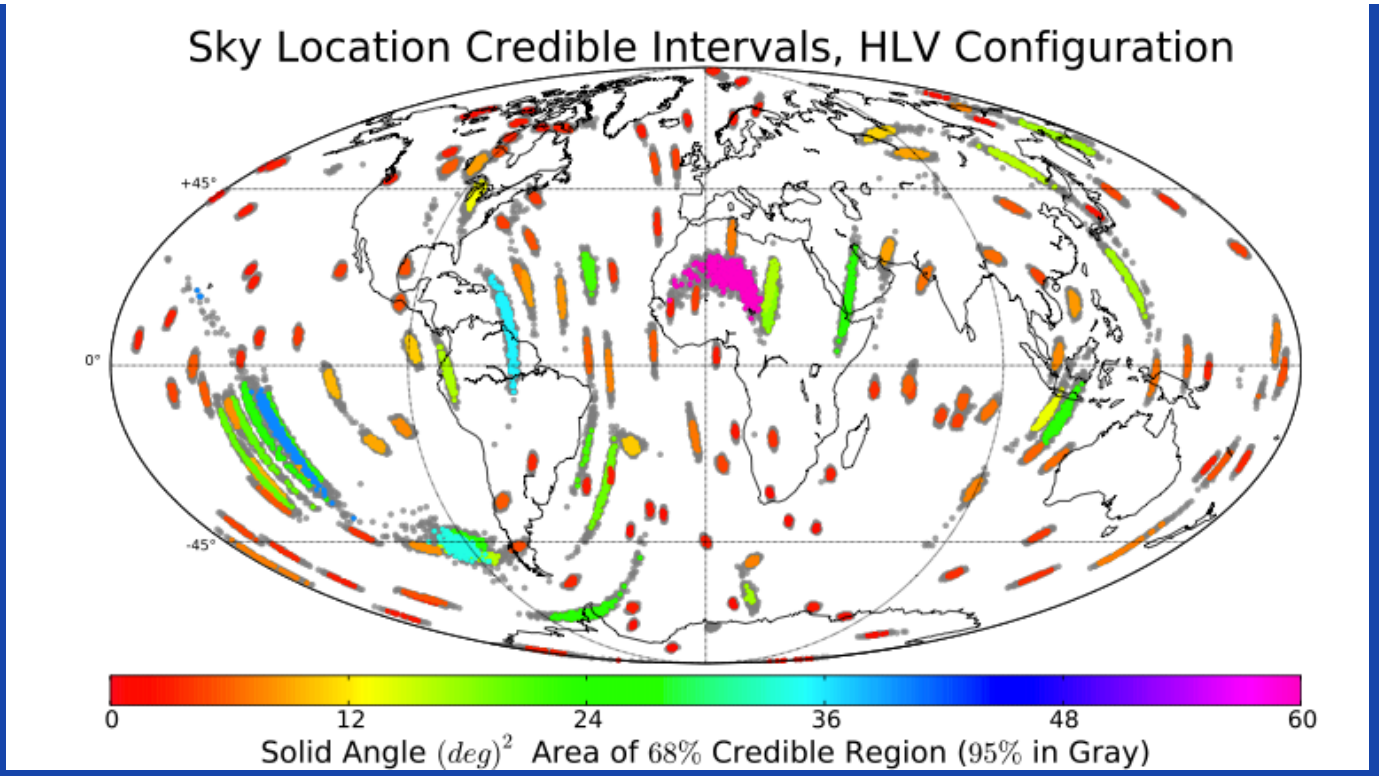

Rodriguez et al. 2014

Importance of EM Detection:

- Improve “confidence” in GW detection; dig deeper into GW data
- Independently constrain binary parameters
- Astrophysical context (e.g. host Galaxy & environment)
- Cosmology (e.g. H_0, w); test strong-field GR; constrain neutron star EOS

Sky Error Regions ~ 10 deg² (~2022)

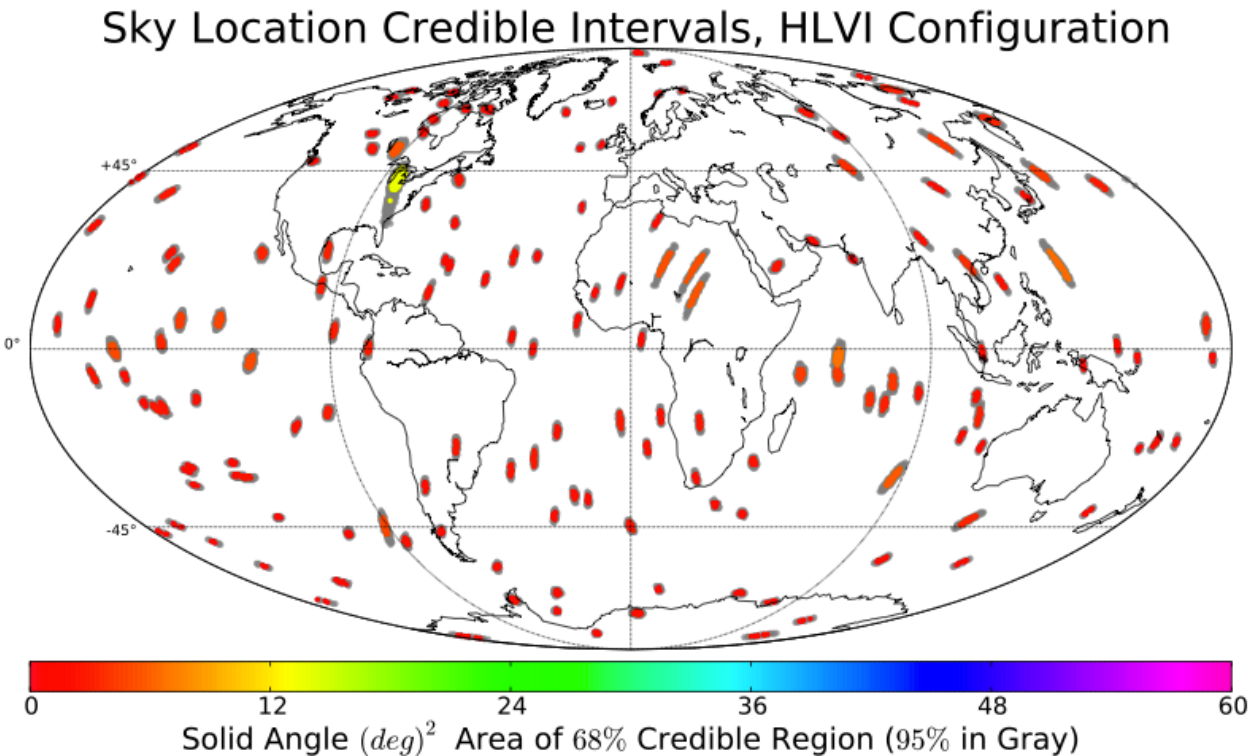

Rodriguez et al. 2014

Numerical Simulation - Two 1.4 $M_\odot$ NSs

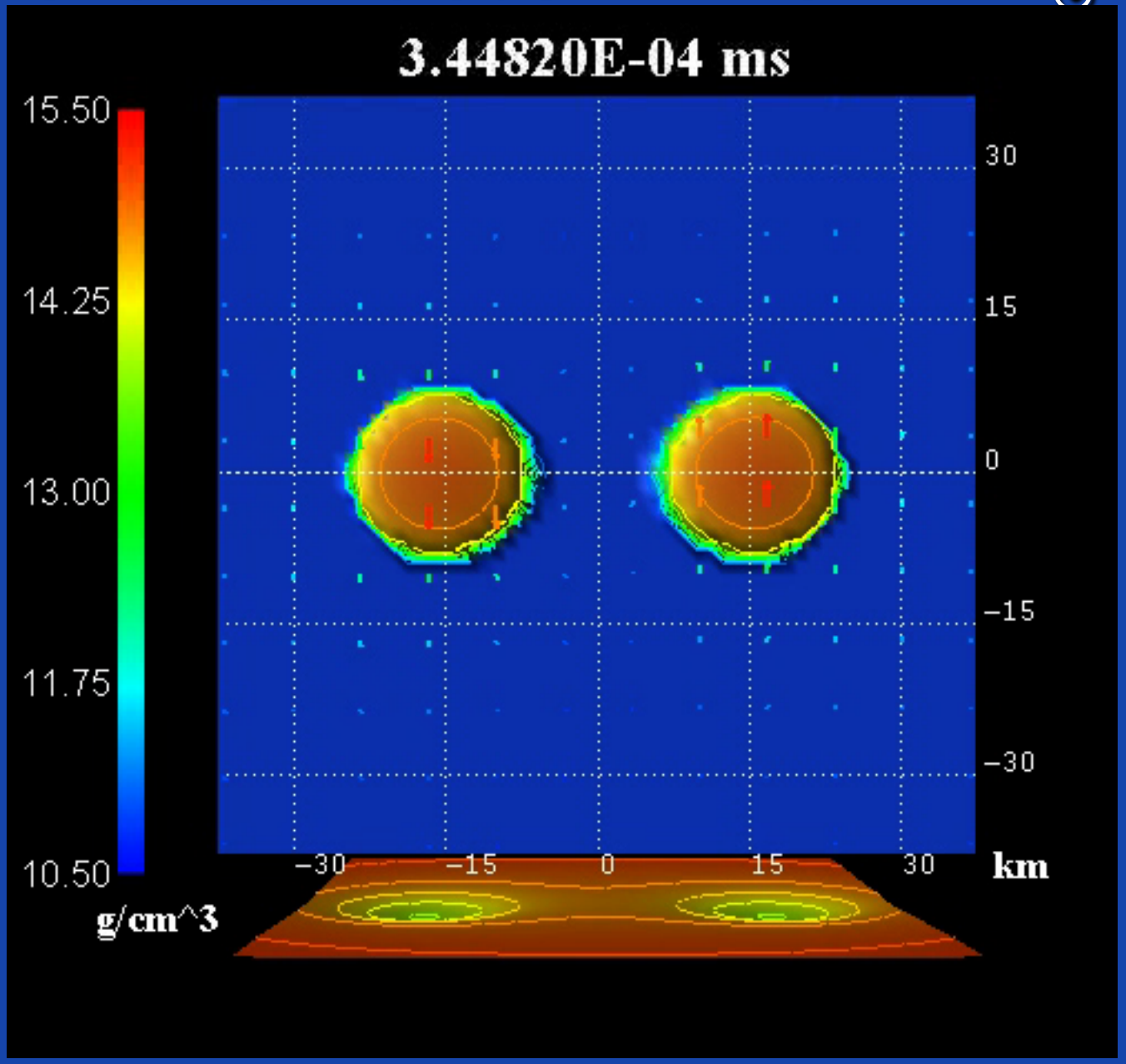

Courtesy M. Shibata (Kyoto)

Electromagnetic Counterparts of NS-NS/NS-BH Mergers

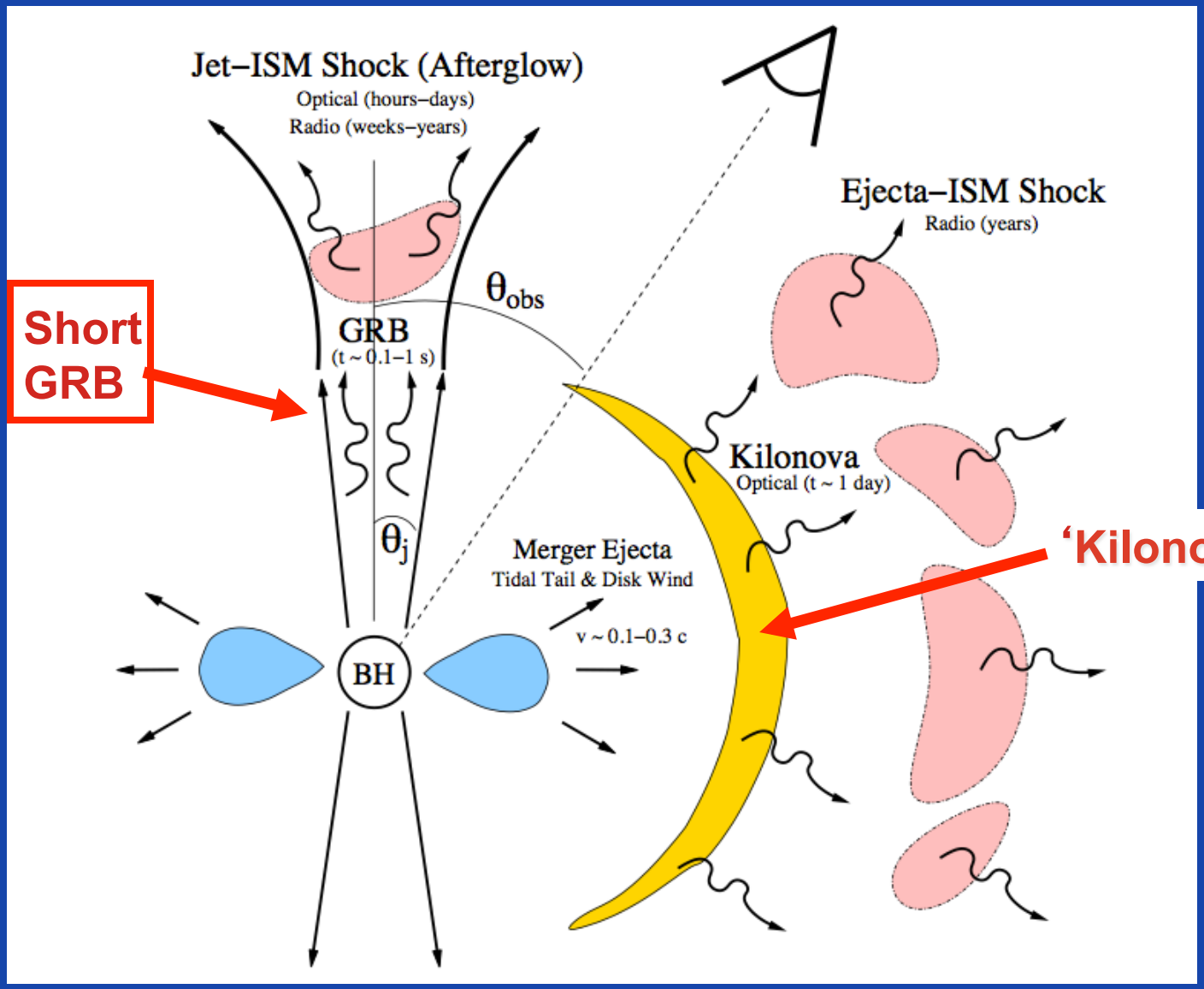

Metzger & Berger 2012

Numerical Simulation - Two 1.4 $M_\odot$ NSs

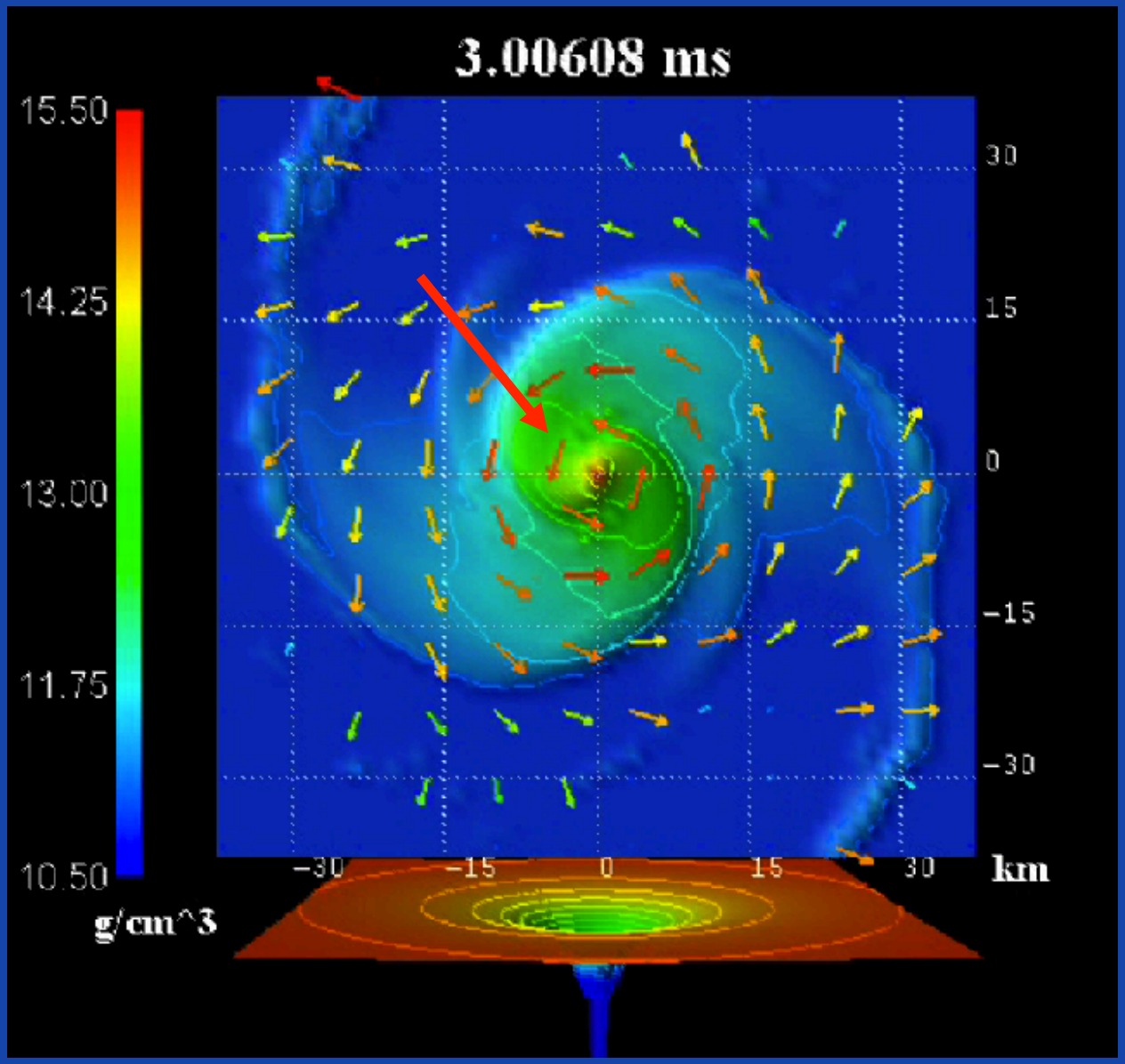

Courtesy M. Shibata (Kyoto)

Short GRBs are Rare in the LIGO Volume

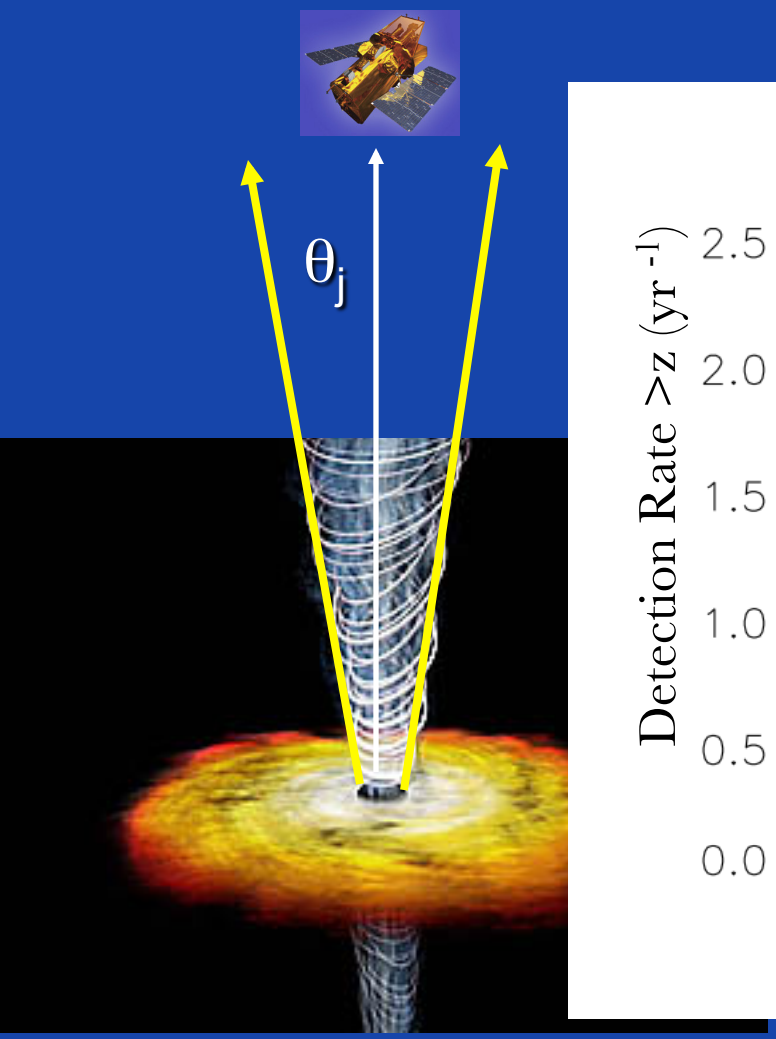

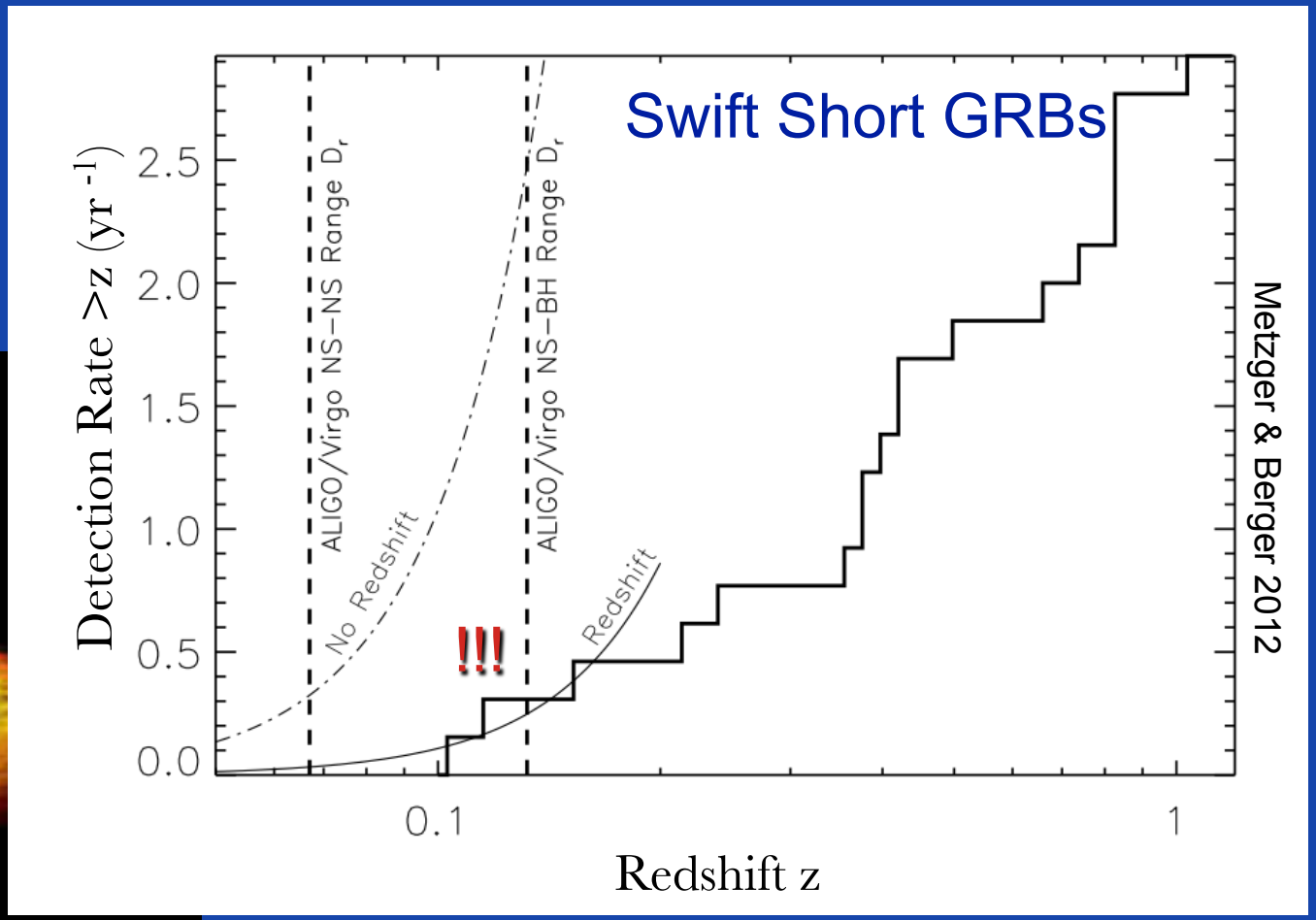

Detectable fraction by all sky γ-ray telescope

$$f_\gamma \sim 3.4 \times \theta_j^2/2 \sim 0.07\left(\frac{\theta_j}{0.2}\right)^2$$

Electromagnetic Counterparts of NS-NS/NS-BH Mergers

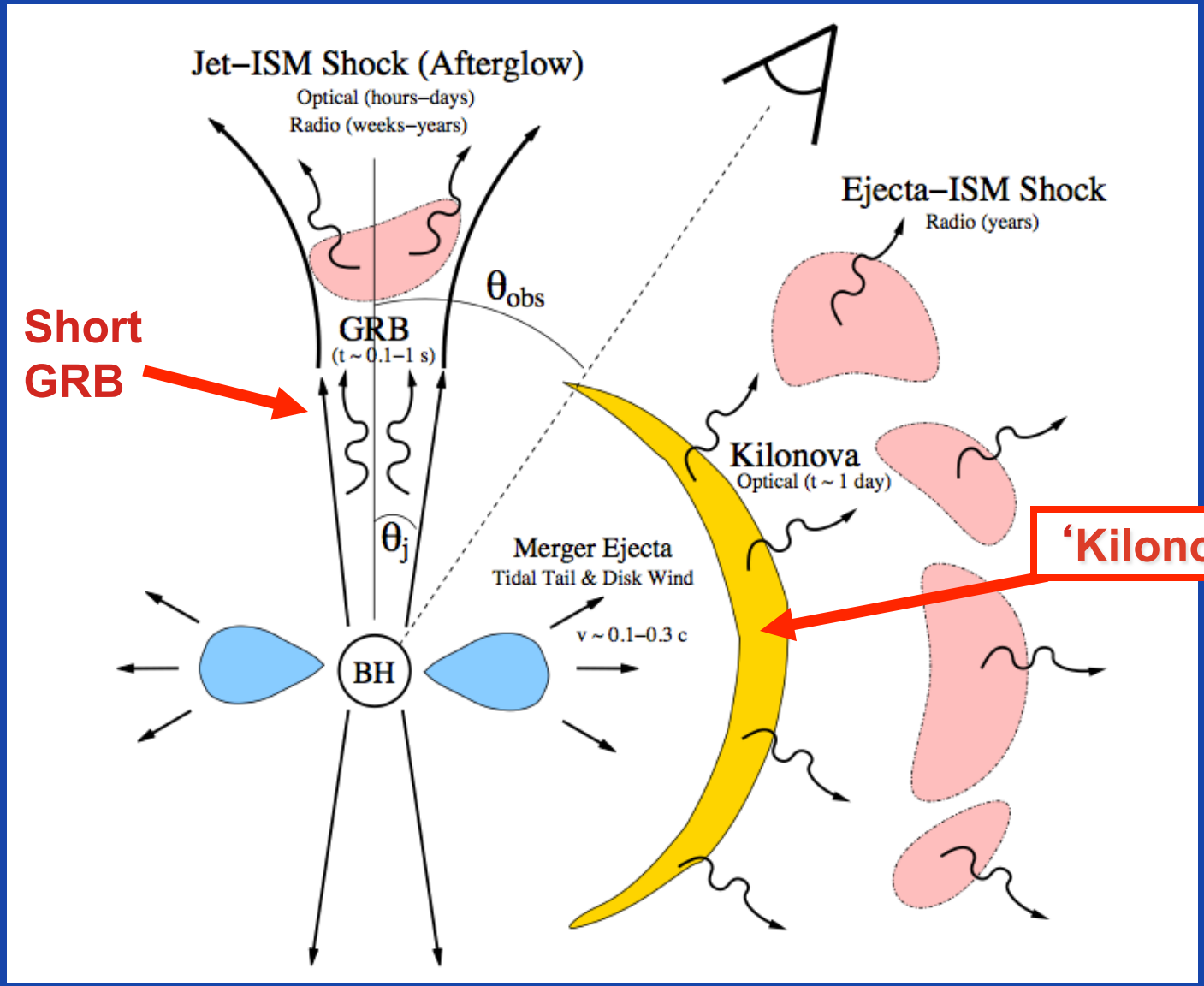

Metzger & Berger 2012

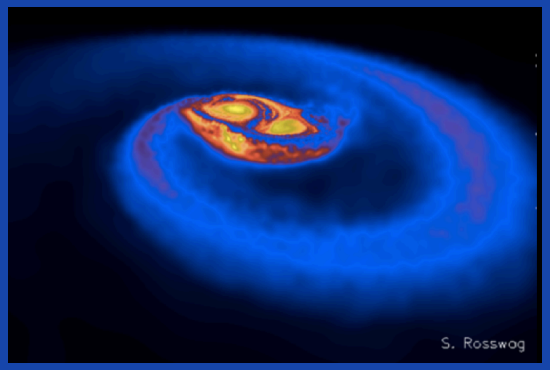

Dynamical Tidal Tails

(e.g. Janka et al. 1999; Rosswog 2005; Shibata & Taniguchi 2006; East et al. 2012; Hotokezaka et al. 2013)

$M_{ej} \sim 10^{-3} - 10^{-2}\ M_\odot$

Model		M_{ej} ($10^{-3}\ M_\odot$)	
APR4-130160	1.8	BH	2.0
APR4-140150	1.8	BH	0.6
APR4-145145	1.8	BH	0.1
APR4-130150	1.8	HMNS→BH	12
APR4-140140	1.8	HMNS→BH	14
APR4-120150	1.6	HMNS	9
APR4-120150	1.8	HMNS	8
APR4-120150	2.0	HMNS	7.5
APR4-125145	1.8	HMNS	7
APR4-130140	1.8	HMNS	8
APR4-135135	1.6	HMNS	11
APR4-135135	1.8	HMNS	7
APR4-135135	2.0	HMNS	5
APR4-120140	1.8	HMNS	3
APR4-125135	1.8	HMNS	5
APR4-130130	1.8	HMNS	2
ALF2-140140	1.8	HMNS→BH	2.5
ALF2-120150	1.8	HMNS	5.5
ALF2-125145	1.8	HMNS	3
ALF2-130140	1.8	HMNS → BH	1.5
ALF2-135135	1.8	HMNS → BH	2.5
ALF2-130130	1.8	HMNS	2
H4-130150	1.8	HMNS→BH	3
H4-140140	1.8	HMNS→BH	0.3
H4-120150	1.6	HMNS	4.5
H4-120150	1.8	HMNS	3.5
H4-120150	2.0	HMNS	4
H4-125145	1.8	HMNS	2
H4-130140	1.8	HMNS	0.7
H4-135135	1.6	HMNS→BH	0.7
H4-135135	1.8	HMNS→BH	0.5
H4-135135	2.0	HMNS	0.4
H4-120140	1.8	HMNS	2.5
H4-125135	1.8	HMNS	0.6
H4-130130	1.8	HMNS	0.3
MS1-140140	1.8	MNS	0.6
MS1-120150	1.8	MNS	3.5
MS1-125145	1.8	MNS	1.5
MS1-130140	1.8	MNS	0.6
MS1-135135	1.8	MNS	1.5
MS1-130130	1.8	MNS	1.5

Hotokezaka et al. 2013

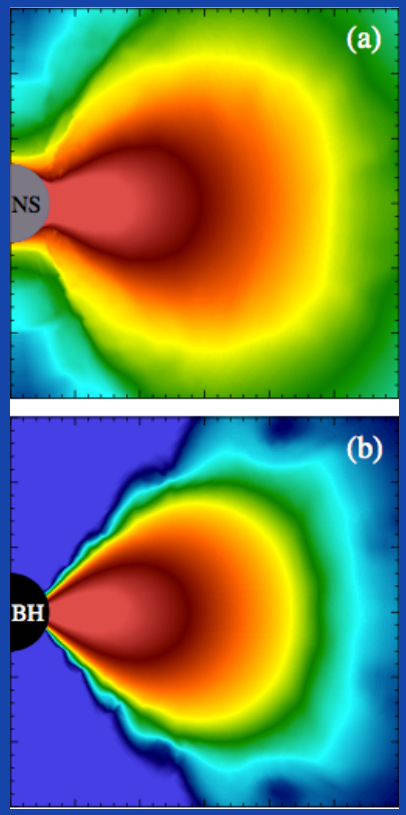

Metzger & Fernandez 2014

Disk Outflows

Neutrino-Powered (Early)

(e.g. McLaughlin & Surman 05; Surman+08; BDM+08; Dessart+09)

Recombination-Powered (Late)

(e.g. Beloborodov 08; BDM+08, 09; Lee+09; Fernandez & BDM 13, 14)

$M_{ej} = f_w M_d \sim 10^{-3}\text{-}10^{-2}\ (f_w/0.1)\ M_\odot$

R-Process Network (neutron captures, photo-dissociations, α- and β-decays, fission)

Final Abundance Distribution

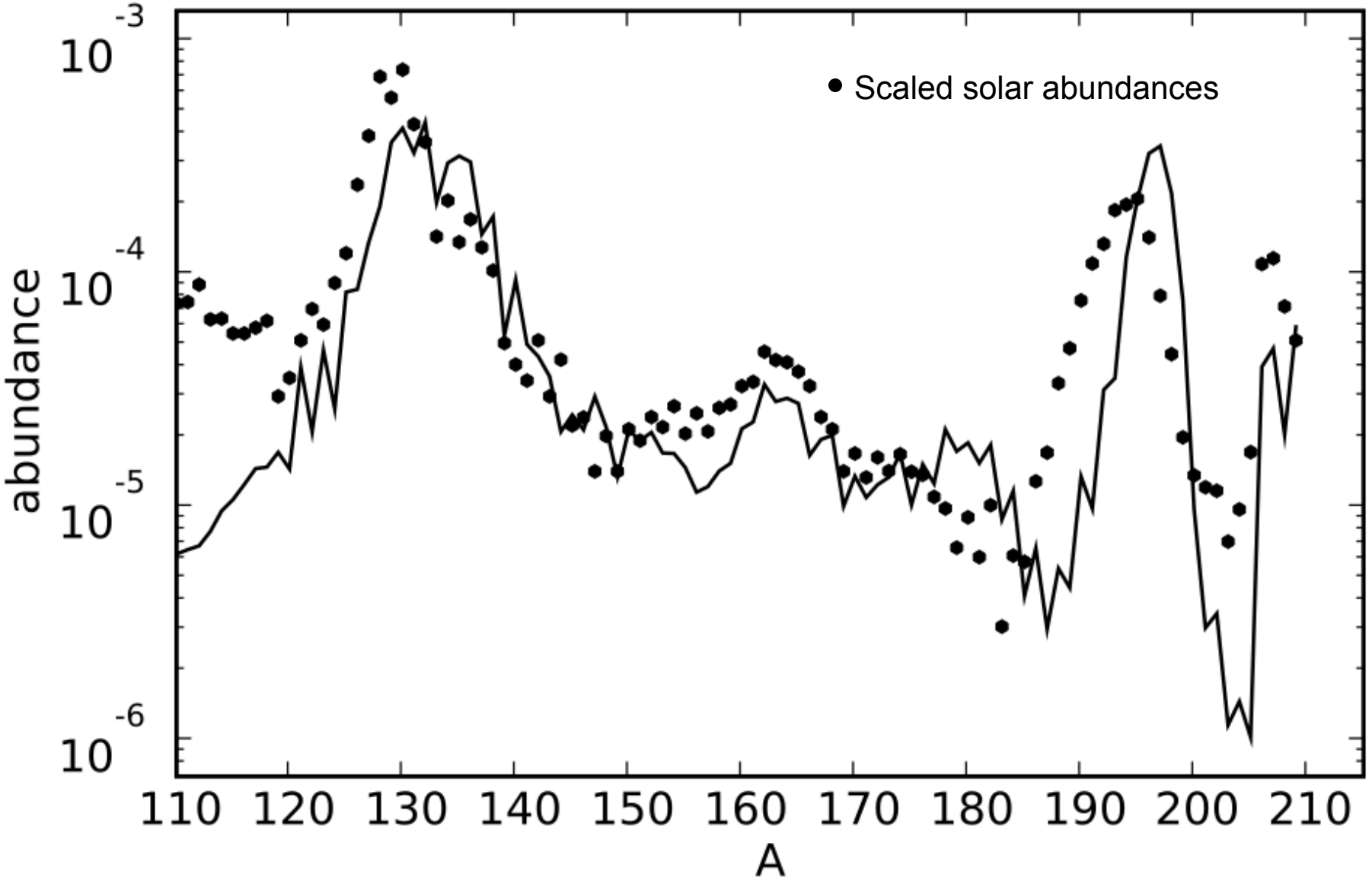

Radioactive Heating of Merger Ejecta

(BDM et al. 2010; Roberts et al. 2011; Goriely et al. 2011; Korobkin et al. 2012; Bauswein et al. 2013)

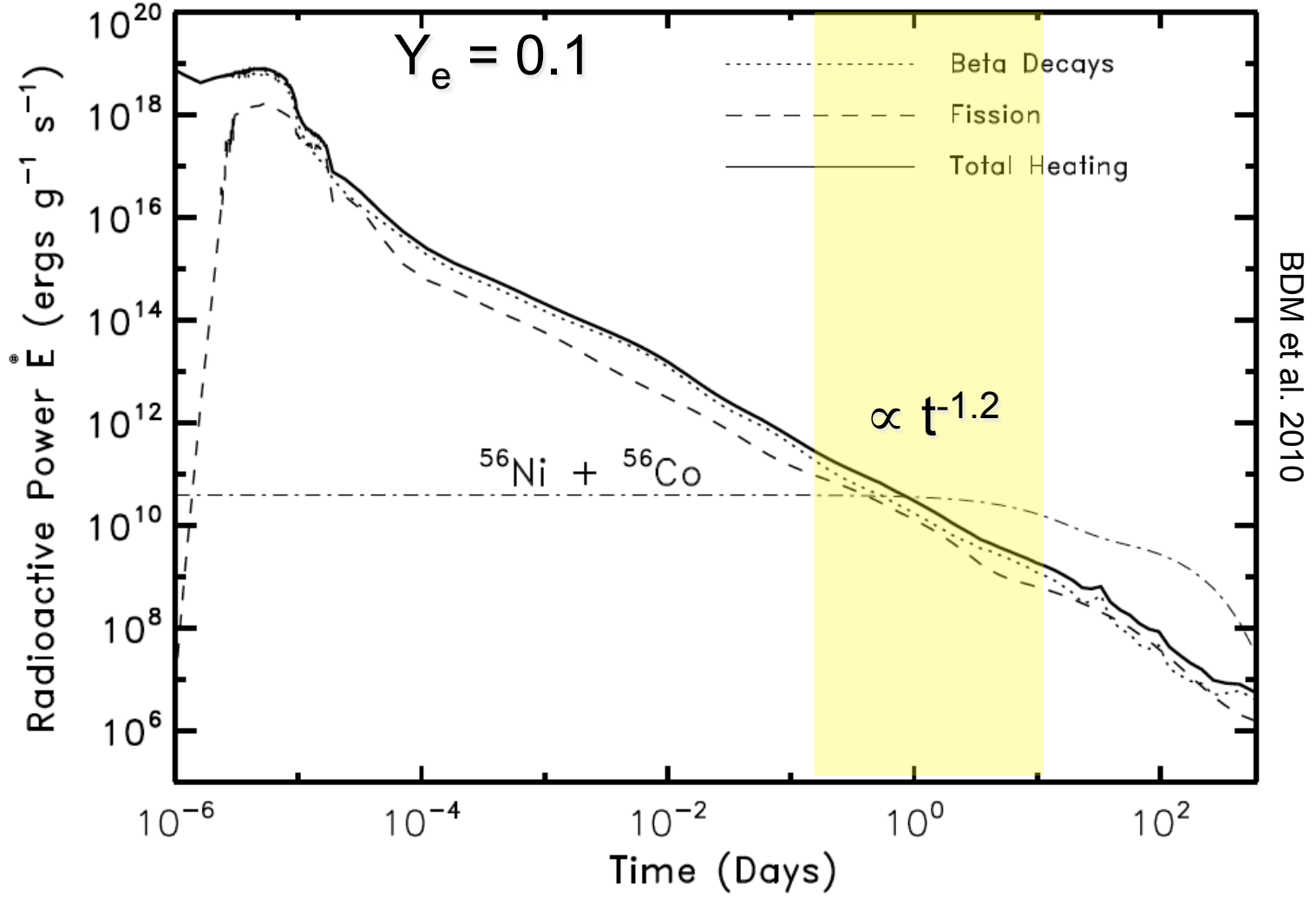

Dominant β-decays at 1 day: ^{132,134,135}I, ^{128,129}Sb,^{129}Te,^{135}Xe

Insensitive to details (Y_e, expansion history, NSE or not)

How Supernovae Shine (Arnett 1982; Li & Paczynski 1998)

spherical ejecta - mass M, velocity v, thermal energy $E = f Mc^2$, & opacity κ

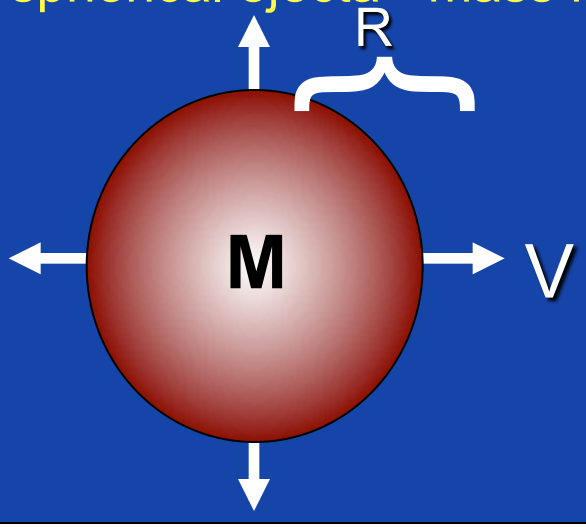

$$R = v\,t \qquad \rho = \frac{M}{4\pi/3\,R^3}$$

$$\tau \sim \kappa\rho R \qquad t_{diff} \sim \tau R/c$$

$$t \sim t_{diff} \Rightarrow \text{peak emission} \quad t_{peak} \sim 2 \text{ weeks} \left(\frac{v}{10^4 \text{ km s}^{-1}}\right)^{-1/2} \left(\frac{M}{M_\odot}\right)^{1/2} \left(\frac{\kappa}{\kappa_{Fe}}\right)^{1/2}$$

$$L_{peak} \sim \frac{E(t_{peak})}{t_{peak}} \sim 10^{43} \text{ ergs s}^{-1} \left(\frac{f}{10^{-5}}\right)\left(\frac{v}{10^4 \text{ km s}^{-1}}\right)^{1/2} \left(\frac{M}{M_\odot}\right)^{1/2} \left(\frac{\kappa}{\kappa_{Fe}}\right)^{-1/2}$$

Type Ia Supernova:

$v \sim 10^4$ km s^{-1}, $M_{ej} \sim M_\odot$, $f_{Ni \to Co} \sim 10^{-5} \Rightarrow t_{peak} \sim$ week, $L \sim 10^{43}$ erg s^{-1}

NS Merger:

$v \sim 0.1$ c, $M_{ej} \sim 10^{-2}\, M_\odot$, $f \sim 10^{-6} \Rightarrow t_{peak} \sim 1$ day, $L \sim 3\ 10^{41}$ erg s^{-1}

"Kilo"-nova Light Curves

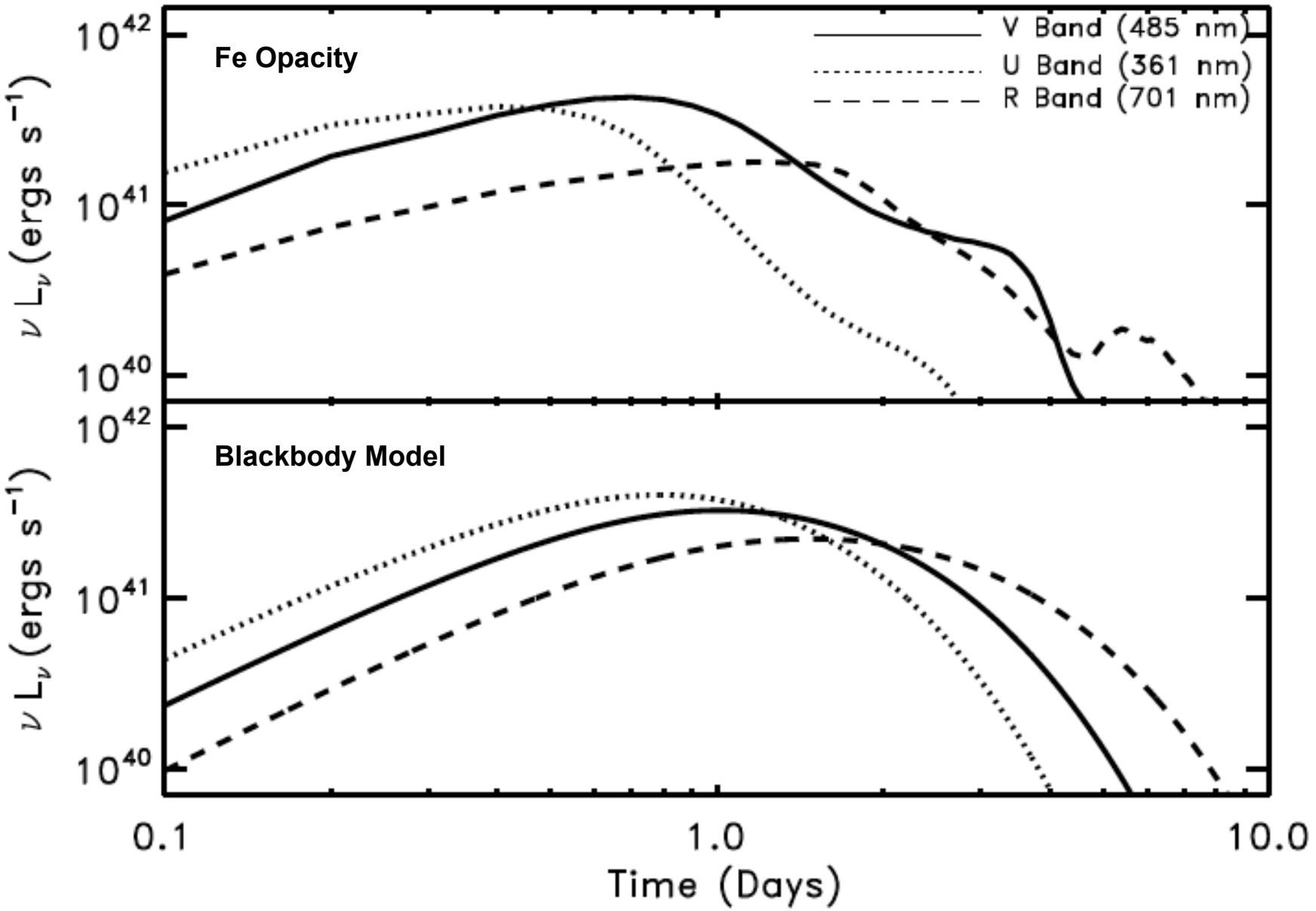

Metzger et al. (2010)

High Opacity of the Lanthanides

(Kasen et al. 2013; Barnes & Kasen 2013)

s-shell (g=2)

$$N_{\rm lev} \sim \frac{g!}{n!(g-n)!}$$

$$N_{\rm lines} \sim N_{\rm lev}^2$$

p-shell (g=6)

d-shell (g=10)

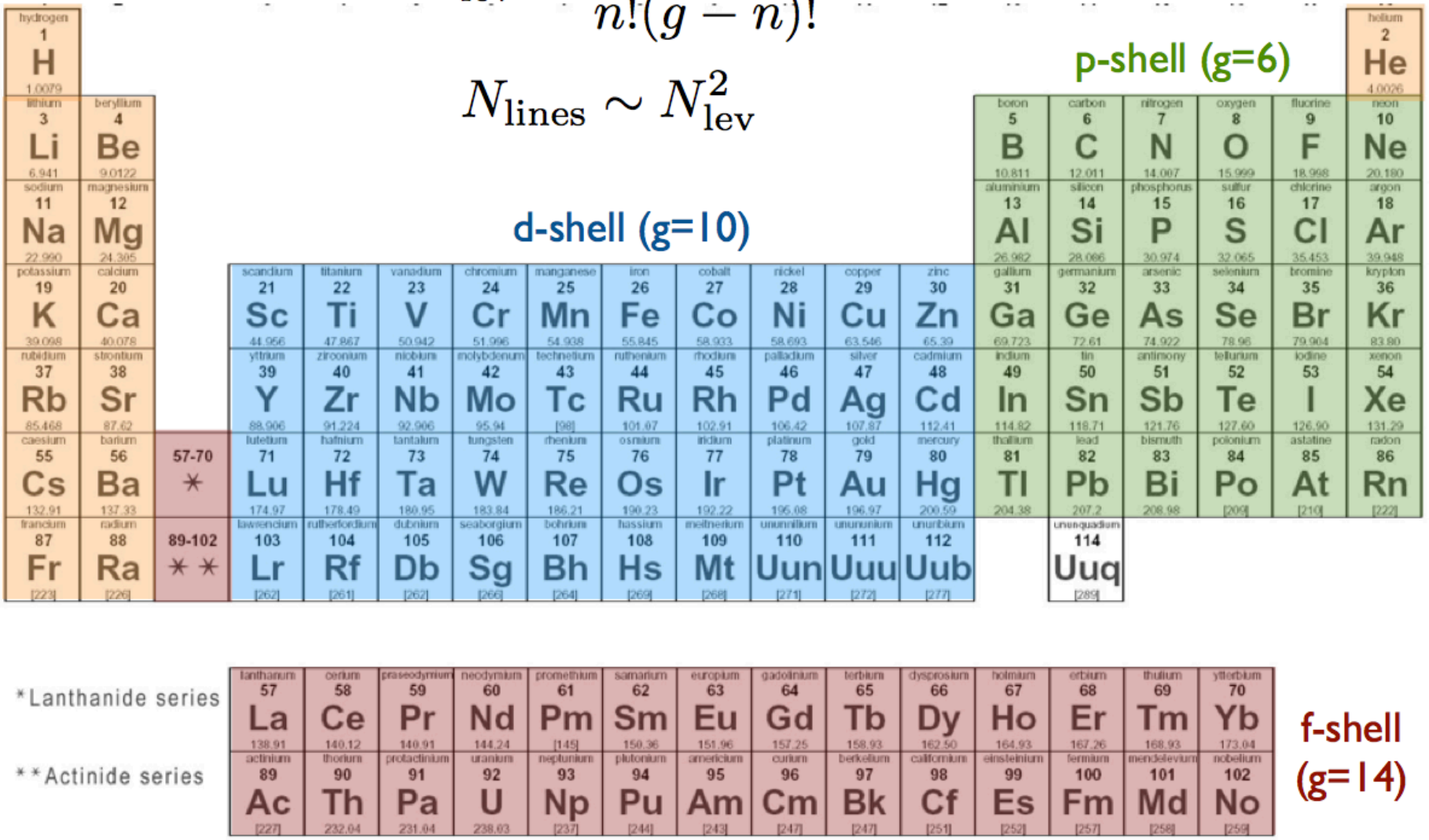

f-shell (g=14)

Slide courtesy D. Kasen

High Opacity of the Lanthanides

(Kasen et al. 2013; Barnes & Kasen 2013)

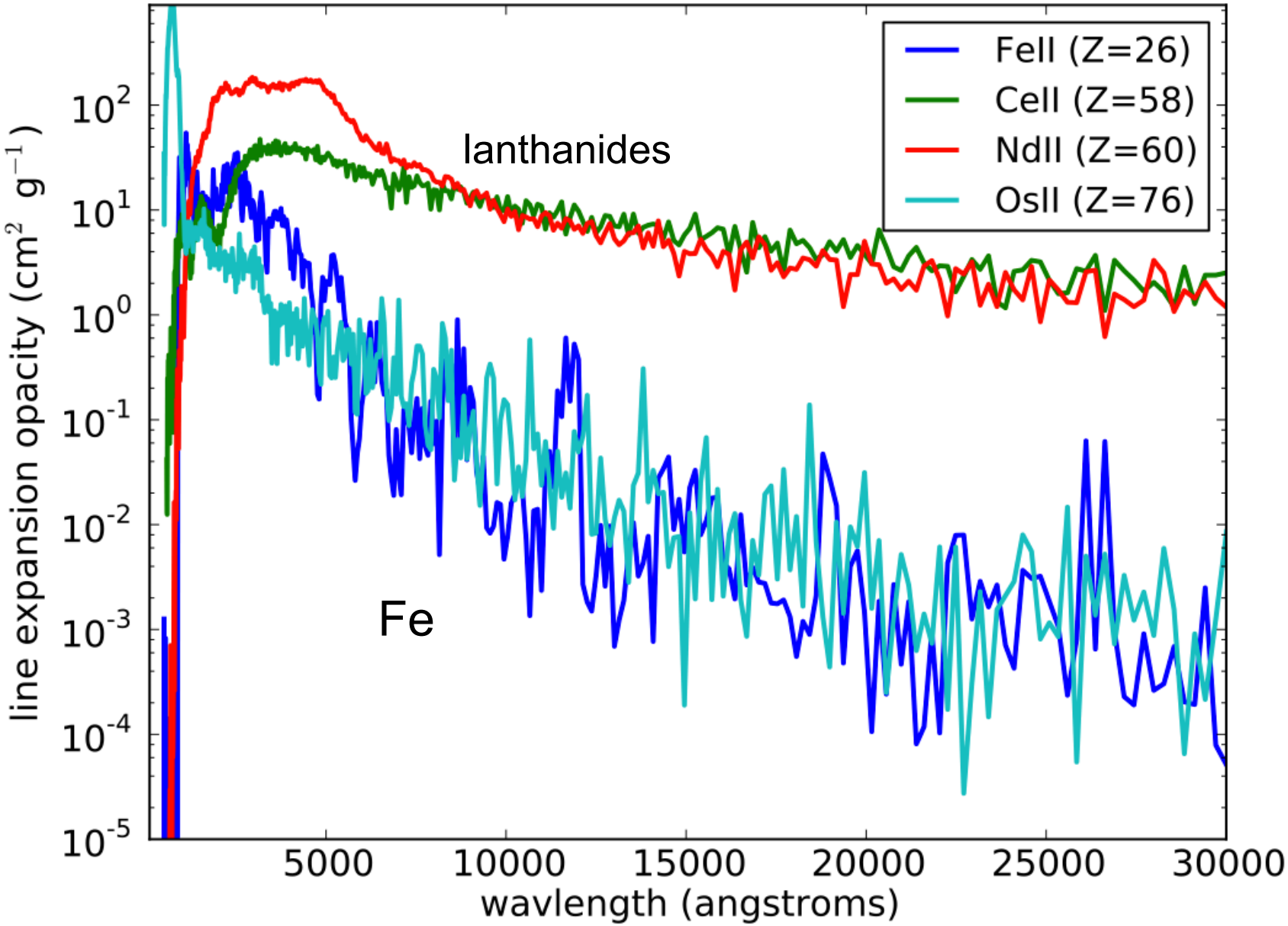

Kasen et al. 2013

light curves of radioactive transients

effect of high lanthanide opacity

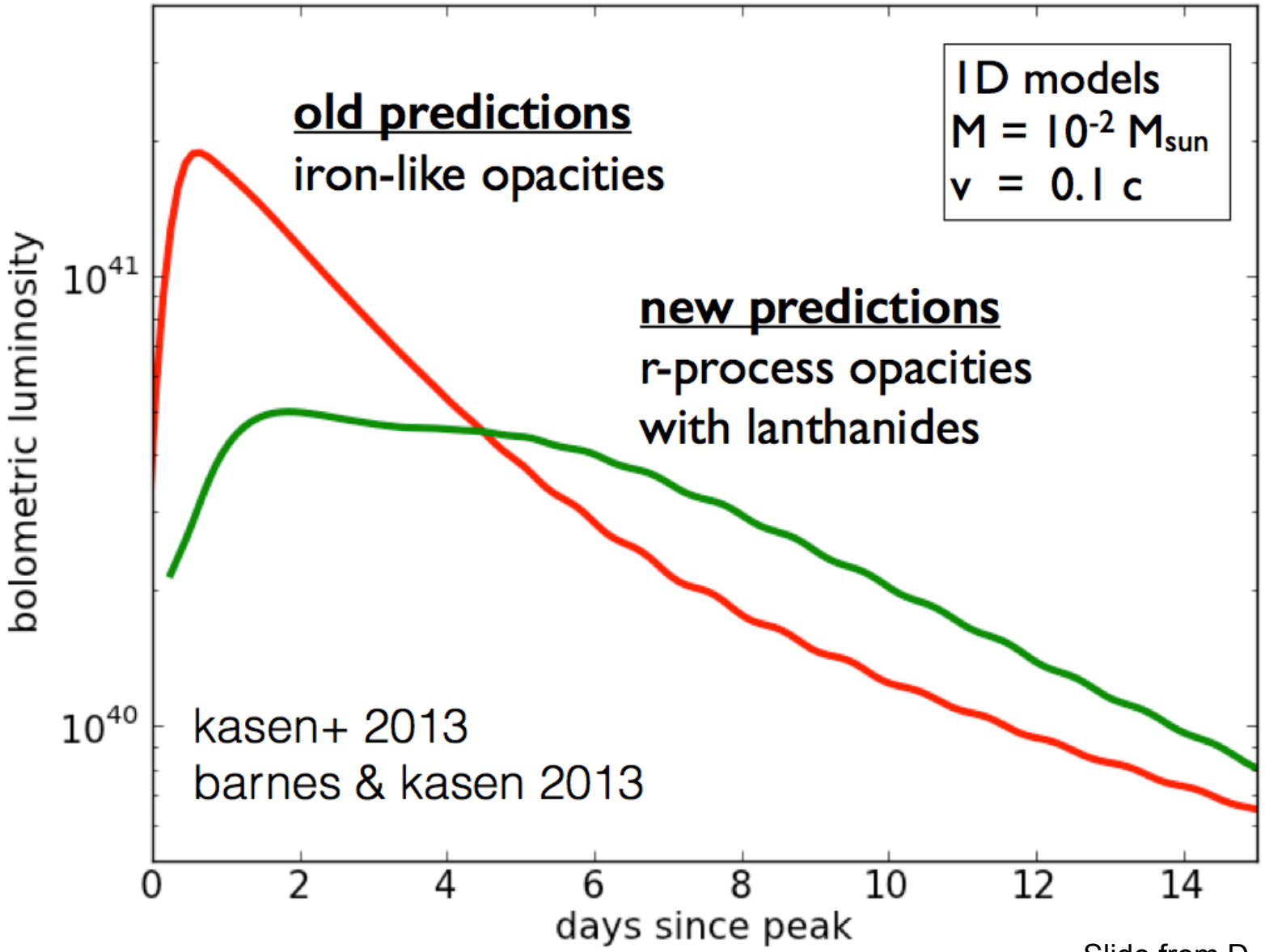

Slide from D. Kasen

AN R-PROCESS KILONOVA ASSOCIATED WITH THE SHORT-HARD GRB 130603B

E. BERGER[1], W. FONG[1], AND R. CHORNOCK[1]

A 'kilonova' associated with the short-duration γ- ray burst GRB 130603B

N. R. Tanvir, A. J. Levan, A. S. Fruchter, J. Hjorth, R. A. Hounsell, K. Wiersema & R. L. Tunnicliffe

Tanvir et al. 2013

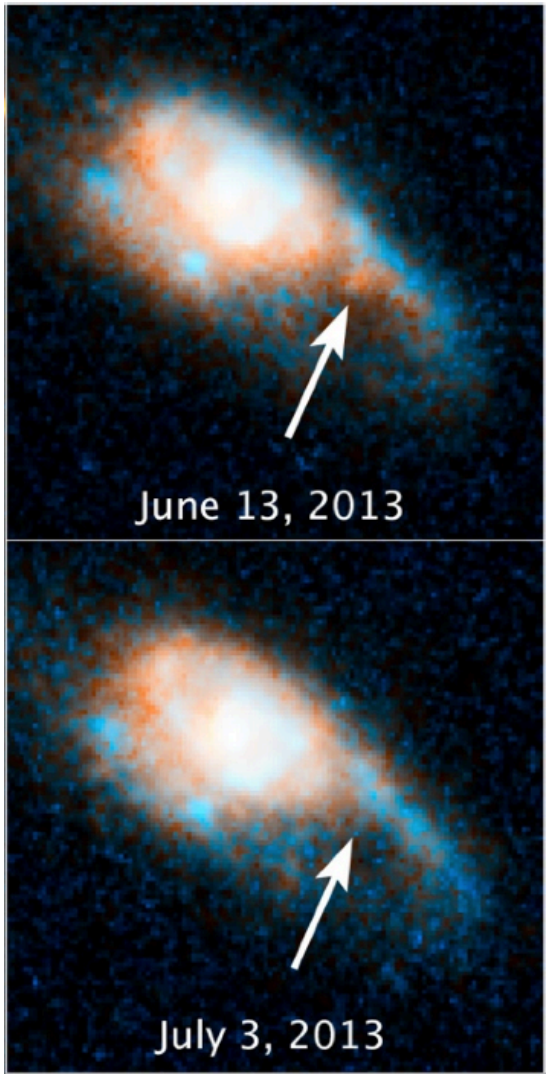

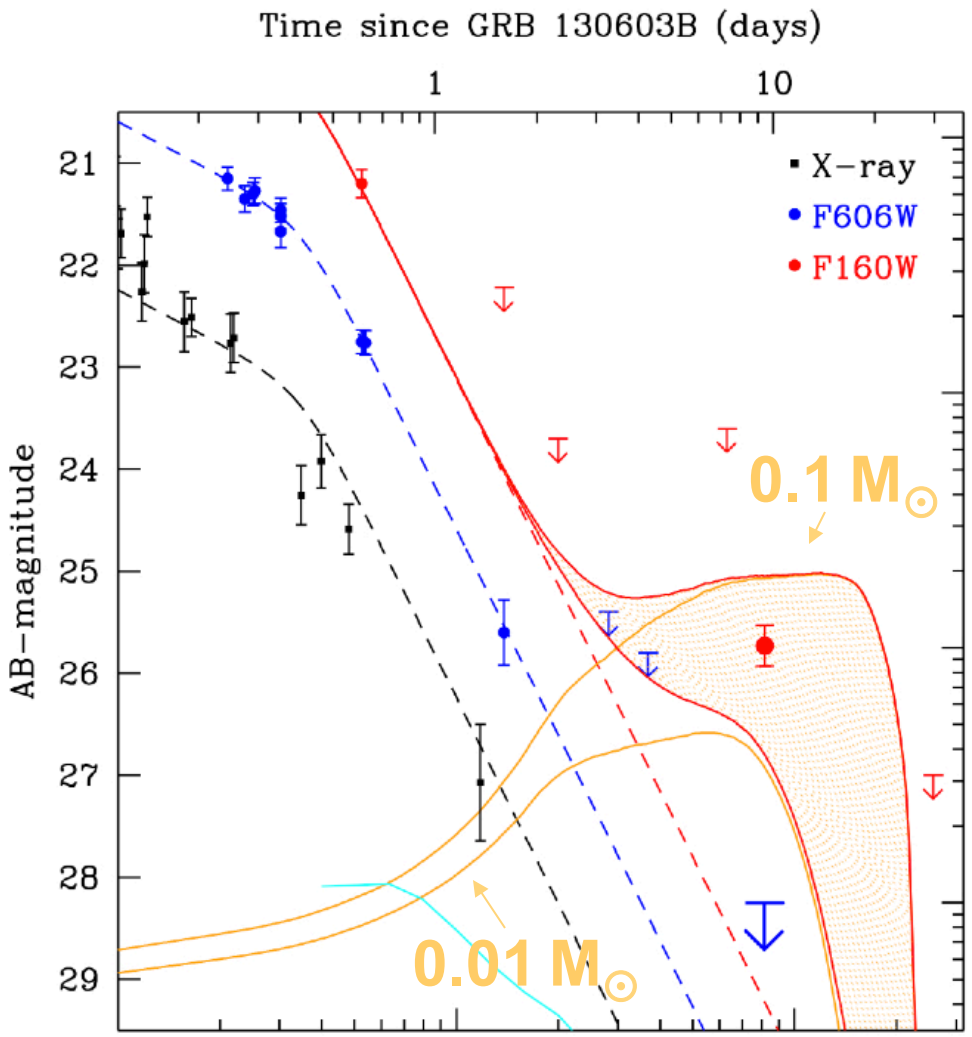

Gravitational Wave Follow-Up

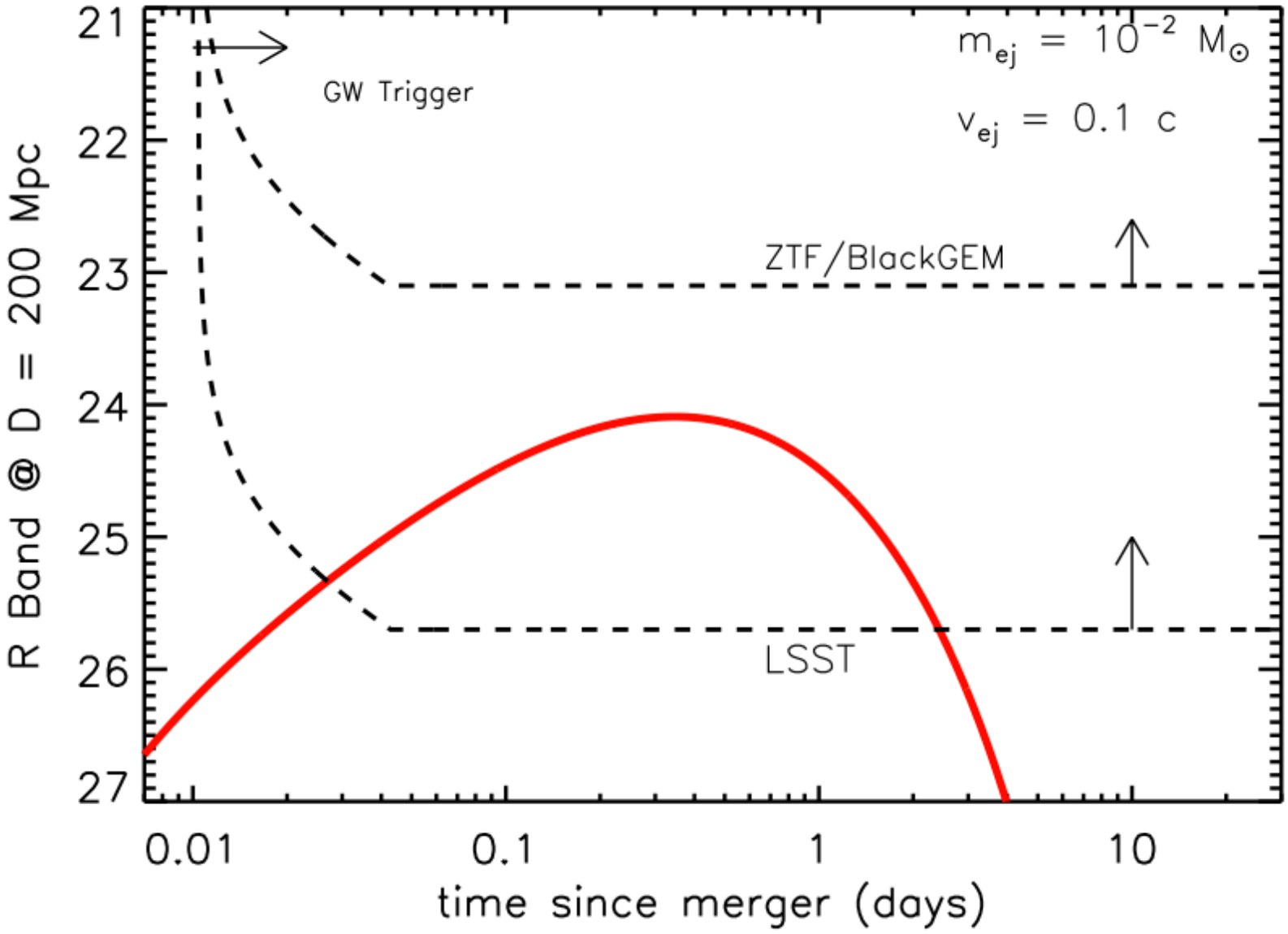

Gravitational Wave Follow-Up

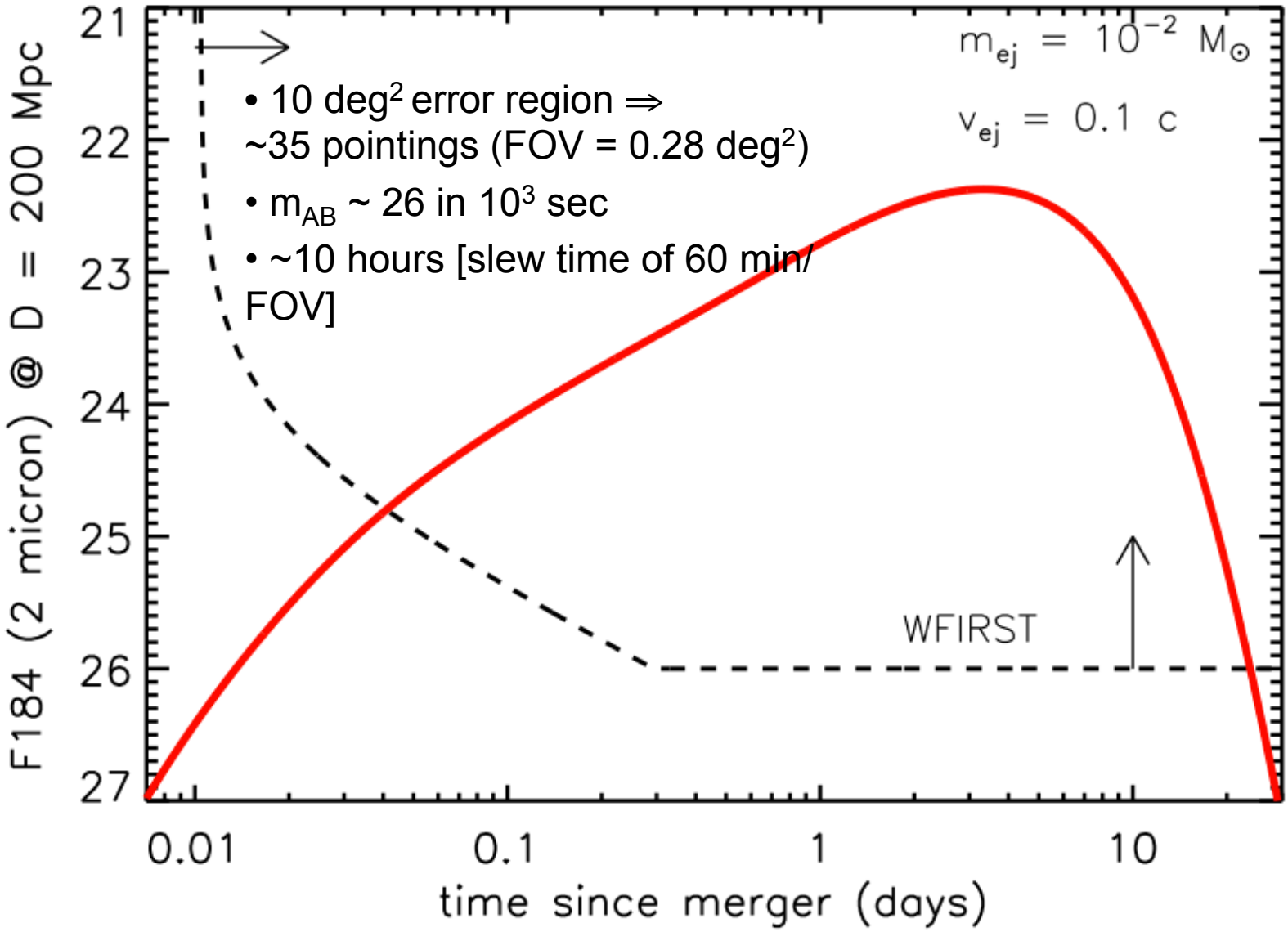

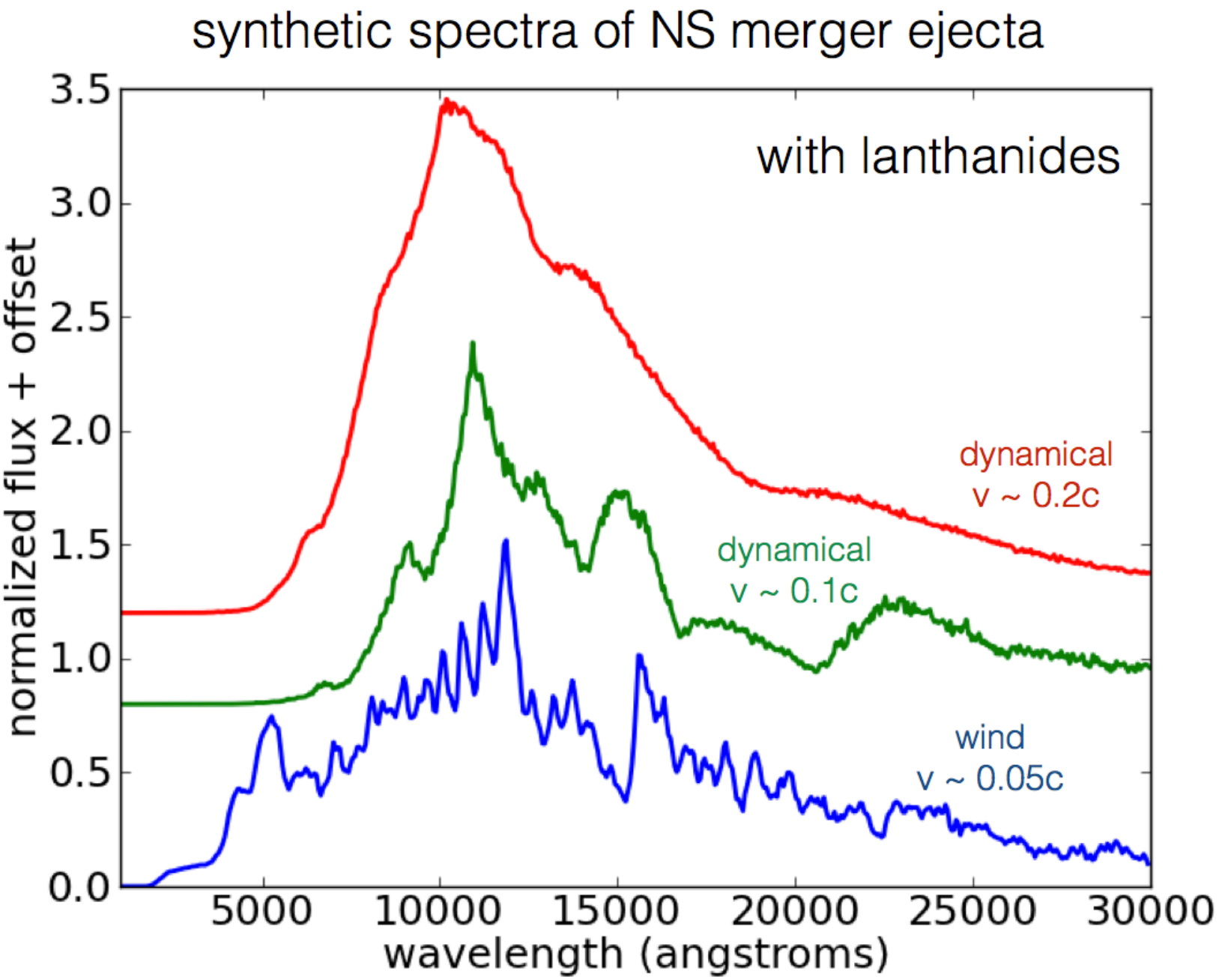
synthetic spectra of NS merger ejecta
with lanthanides
dynamical
v ~ 0.2c
dynamical
v ~ 0.1c
wind
v ~ 0.05c
normalized flux + offset
wavelength (angstroms)
0.0
0.5
1.0
1.5
2.0
2.5
3.0
3.5
5000
10000
15000
20000
25000
30000

Conclusions

- The first direct detection of gravitational waves will likely be a binary NS merger, within the next ~3 years. ***Identifying an EM counterpart will be essential to maximize the scientific impact of this discovery.***
- The most promising isotropic counterpart is an optical / NIR transient ("kilonova") powered by the radioactive decay of r-process nuclei.
- The high opacity opacity of neutron-rich matter causes the kilonova SED to peak in the near infrared.
- First kilonova possibly detected following GRB 130603B last June, confirming the association of mergers with short GRBs.
- Kilonovae directly probe the formation of r-process nuclei, a long standing mysteries in nuclear astrophysics, and physical processes at work during the merger, such as the delay until black hole formation
- The wide FoV and NIR sensitivity of WFIRST make it an ideal tool for gravitational wave follow-up in the coming Advanced LIGO/Virgo era.